UV Absorption Spectrum and Rate Constant for Self-Reaction of Silyl Radicals

Alexey V. Baklanov[†] and Lev N. Krasnoperov*

Department of Chemical Engineering, Chemistry and Environmental Science, New Jersey Institute of Technology, University Heights, Newark, New Jersey 07102

Received: November 14, 2000; In Final Form: February 26, 2001

The rate constant of self-reaction of silyl radicals, $SiH_3 + SiH_3 \rightarrow$ products (1), was measured at 300 K over an extended buffer gas pressure range (1−100 bar, He) using excimer laser pulsed photolysis combined with the transient UV spectroscopy. Silyl radicals were produced in fast reaction of chlorine atoms with silane, $Cl + SiH_4 \rightarrow SiH_3 + HCl$. Oxalyl chloride, $(COCl)_2$, and phosgene, $COCl_2$, were used as "clean" photodissociation sources of Cl atoms at 193 nm (ArF laser). Silyl radicals were monitored using UV absorption. The absorption cross-sections of SiH_3 radicals are determined using the measured photodepletion of the precursor, $(COCl)_2$, via its transient absorption at 210 nm. The UV absorption of silyl radical has maximum at 218 nm with the absorption cross-section, $\sigma_{SiH3}(218\ nm) = (2.01 \pm 0.11) \times 10^{-17}$ cm^2 molecule^{-1}. No pressure dependence of the overall rate constant of reaction 1 was found over the range 1−100 bar (He). The measured rate constant is: $k_1 = (8.25 \pm 1.05) \times 10^{-11}$ cm^3 molecule^{-1} s^{-1} at 300 K. Observed residual UV absorption, tentatively assigned to the dissociation products of the vibrationally excited Si_2H_6* molecules formed in reaction 1, is quenched by the buffer gas at 100 bar pressure due to the collisional stabilization of excited disilane molecules.

Introduction

Silyl radical, SiH_3, is an important intermediate in the mechanisms of the gas-phase chemical transformations of silicon containing molecules. The radical plays a role similar to that of methyl radical in hydrocarbon reactions. Silicon-centered transient species are the key intermediates in the silicon and silicon-containing thin film chemical vapor deposition (CVD) processes.[1] CVD produced thin silicon-containing films are used in microelectronics as well as protective coatings.[1−3] Since the first detection of silyl radical in the gas phase[4−7] and the first direct study of elementary reactions of this radical,[8,9] there has been significant progress in the accumulation of rate data for this important intermediate. Direct kinetic studies of reactions of small silicon hydride radicals have been recently reviewed.[10] These studies provided a significant body of rate constant data as well as (via the equilibrium constant determination) the Si−H and Si−N bond energies in SiH_4, $Si(CH_3)_3H$, $Si(CH_3)_3NO$, and SiH_3NO.[11−14]

Self-reaction of silyl radicals (reaction 1) is one of the important reactions of this radical. In contrast to its hydrocarbon analogue, reaction of recombination of methyl radicals, self-reaction of silyl radicals has more complex mechanism due to the existence of two open channels for dissociation of the energized adduct formed in the initial recombination step[15]

$$SiH_3 + SiH_3 \rightarrow Si_2H_6^* \quad (1a)$$

$$Si_2H_6^* \rightarrow SiH_4 + SiH_2 \quad (1b)$$

$$Si_2H_6^* \rightarrow HSiSiH_3 + H_2 \quad (1c)$$

$$Si_2H_6^* + M \rightarrow Si_2H_6 + M \quad (1d)$$

$$SiH_3 + SiH_3 \rightarrow SiH_2 + SiH_4 \quad (1e)$$

In this mechanism, Si_2H_6* represents energized disilane molecule, which is formed in the recombination step 1a. The energy of this energized molecule is sufficient for the dissociation via channels 1b and 1c.[15] In addition, disilane is formed when energized molecules are deactivated in collisions with bath gas molecules (reaction 1d). The channel 1e represents the direct abstraction reaction.

Reaction 1 was extensively studied using different experimental techniques. In the first study of reaction 1 Itabashi et al.[16] used pulsed electric discharge in silane/hydrogen mixtures to produce silyl radicals and laser infrared absorption spectroscopy to monitor these radicals. The reported rate constant is $(1.5 \pm 0.6) \times 10^{-10}$ cm^3 molecule^{-1} s^{-1}. Although determination of the absolute concentrations of silyl radicals was possible via the calculated strength of the IR transition used, the apparent deficiency of this study is in the possible production and kinetic interference of other reactive species, (such as SiH_2, SiH, H, etc.) All other studies employed the originally suggested[4−9] and widely used later indirect generation of silyl radicals using fast reaction of chlorine atoms with silane molecules[17−24]

$$Cl + SiH_4 \rightarrow HCl + SiH_3 \quad (2)$$

Loh et al.[19] and Loh and Jasinski[20] used excimer laser photolysis at 193 nm to generate chlorine atoms by photolysis of CCl_4. Laser diode spectroscopy was used to monitor silyl radicals. The initial concentrations were derived from the IR absorption measurements of HCl formed in reaction 2. The reported rate constant of reaction 1 is $(7.9 \pm 2.9) \times 10^{-11}$ cm^3 molecule^{-1} s^{-1}. Koshi et al.[21] used the same approach to generate chlorine atoms (ArF laser photolysis of CCl_4), while monitored SiH_3 using electron impact mass-spectrometry. As in refs 19 and 20, the initial concentrations were determined via HCl measurements. The rate constant reported, $(1.2 \pm 0.4) \times 10^{-10}$ cm^3 molecule^{-1} s^{-1}, is somewhat higher than that of Loh and Jasinski and lower than that of Itabashi et al.[16]

Photolysis of CCl_4 produces other reactive species (CCl_3, CCl_2) in addition to chlorine atoms, which might interfere with

* To whom correspondence should be addressed. E-mail: KRASNOPEROV@ADM.NJIT.EDU

[†] On leave from the Institute of Chemical Kinetics and Combustion, Novosibirsk 630090, Russia.

10.1021/jp004198l CCC: $20.00
Published on Web 05/01/2001

the kinetic measurements. To avoid difficulties associated with the formation of other free radical species in generation of atomic chlorine, Baklanov and Chichinin used a clean photolytic source of chlorine atom—excimer laser photolysis of phosgene at 248 nm[22]

$$COCl_2 + h\nu(248\ nm) \rightarrow 2\ Cl + CO \qquad (3)$$

Sensitive time-resolved Laser Magnetic Resonance[8,9] technique was used for direct monitoring of silyl radicals. The rate constant of reaction 1 measured in this study, $(1.6 \pm 0.5) \times 10^{-11}$ cm^3 molecule^{-1} s^{-1} was considerably lower than in the previous determinations. Although a clean source of chlorine atoms was used, no direct determination of the initial concentrations of free radical was attempted due to the relatively small absorption cross-section of phosgene at 248 nm and the difficulties associated with the absolute calibration of the sensitivity of the intra-cavity LMR. Instead, a somewhat complicated and indirect procedure, essentially based on the rate of silyl radical build-up in the excess of chlorine atoms compared to silane, was used.

In a subsequent paper, Matsumoto et al. used another generator of chlorine atoms—ArF laser photolysis of C_2Cl_4.[23] The reaction monitoring was performed using electron impact ionization mass-spectrometry. The determined rate constant, $(9.5 \pm 3.5) \times 10^{-11}$ cm^3 molecule^{-1} s^{-1}, is in agreement with the previous results obtained using photolysis of CCl_4 as a source of chlorine atoms. However, photolysis of C_2Cl_4 also produces additional free radical species, which could potentially interfere in the kinetic measurements.

For these reasons, in this work reaction 1 was reinvestigated using recently developed clean source of chlorine atoms—ArF laser photolysis of oxalyl chloride[25]

$$(COCl)_2 + h\nu(193\ nm) \rightarrow 2\ Cl + 2\ CO \qquad (4)$$

The photolysis of oxalyl chloride quantitatively produces two chlorine atoms and two molecules of carbon monoxide (the photodissociation yield of chlorine atom is 2 within the experimental error[25]). Although this source is similar to the photolysis of phosgene, the advantages of oxalyl chloride lie in its much smaller toxicity and much higher absorption cross-sections in the UV. The latter allows substantial photodepletion of the precursor and reliable determination of the absolute concentration of chlorine atoms using photodepletion measurements, taken by transient UV spectroscopy.

The relative UV-absorption spectrum of silyl radicals was measured by Lightfoot et al.[26] using broadband flash lamp photolysis of CCl_4 as a source of chlorine atoms and reaction 2 to generate silyl radicals. Absolute cross-sections were determined with the accuracy within the factor of 2 due to the uncertainty of the mechanism of CCl_4 photolysis by the broadband light used in the study.[26]

In the course of the current study, the UV absorption of silyl radicals was quantitatively characterized. The rate constant of reaction 1 was measured over an extended buffer gas pressure range, 1−100 bar (He). No pressure dependence of the overall reaction 1 was found within the experimental error. The measured rate constant of reaction 1 is in excellent agreement with the measurements of Loh and Jasinski.[20] The influence of the collisional quenching of the reaction channels 1b and 1c on the reaction branching ratio is demonstrated.

Experimental Section

The experimental approach is based on a combination of pulsed excimer laser photolysis—transient UV−Vis absorption spectroscopy coupled to a high-pressure flow system. The experimental setup is described in detail elsewhere.[25,27] Oxalyl chloride, $(COCl)_2$, and phosgene, $COCl_2$, were used as photolytic precursors of chlorine atoms. The spectroscopic and photochemical characterizations of oxalyl chloride over an extended buffer gas pressure range are described elsewhere.[25] The reactant mixture, which contains Cl-atom precursor (oxalyl chloride, $(COCl)_2$, or phosgene, $COCl_2$), silane, SiH_4, and a buffer gas (He) in great excess (10^3−10^5 times), was flowing through a high-pressure absorption cell. The cell (internal diameter, 7.2 mm; internal length, 10.4 cm; volume, 4.2 cm) was equipped with two thick, fused silica windows and can be used to pressures up to 150 bar. Concentrations of oxalyl chloride were in the range $[(COCl)_2] = (5-6) \times 10^{15}$ molecule cm^{-3}; the concentration of phosgene used was $[COCl_2] = 3 \times 10^{16}$ molecule cm^{-3}. The typical energy flux of the ArF excimer laser light ($\lambda = 193$ nm) was ca. 20 mJ cm^{-2}. With the precursor concentrations used the absorption of the ArF laser light along the reactor length was about 20%. In the majority of the experiments, the silane concentration in the reactor was in the range $[SiH_4] = (1-15) \times 10^{16}$ molecule cm^{-3}. The initial concentrations of chlorine atoms generated by the laser pulse were $[Cl]_0 = (7-8) \times 10^{14}$ molecule cm^{-3}. All experiments were performed at ambient temperature, 300 ± 3 K, and five buffer gas pressures: 1, 3, 10, 30, and 101 bar. Helium was used as a buffer gas. The experiments were performed under the conditions of complete replacement of the reaction mixture between the laser pulses using proper gas flows (3−60 standard cubic centimeter per second) and repetition rates (such as 0.5 Hz at 1 bar and 0.1 Hz at 100 bar).

Hollow cathode lamps (HCL) as well as a low-power Xe arc lamp (75 W) were used as sources of the monitoring light. To improve the monitoring light intensity, a three-electrode hollow cathode lamp (Superlamp, Photron), with square pulses at 4 Amp current and 3 ms duration, was used with current boosting. The light from a light source (hollow cathode lamp or Xe arc lamp) was focused into the cell and then onto the entrance slit of a grating monochromator (Jarrell-Ash, Model 82-518, 0.5 m) using two fused silica lenses with the focal lengths of 10 cm.

The spatial overlap of the light of ArF excimer laser (Lumonics TE−861T-3) with the probing beam of HCL in the cell was arranged using a 45° dielectric mirror (> 98% at 193 nm, Newport). The mirror reflects almost all light at 193 nm, whereas it is transparent for the probing radiation. Unfocused beam of ArF excimer laser filled all the cross-section of the cell to provide near-uniform radiation flux conditions and, therefore, a near-uniform initial Cl atoms concentration profile. After passing the cell, the laser beam was separated from the monitoring light using a similar 45° dielectric mirror for 193 nm. The spaces between the laser light coupling dielectric mirrors and the reaction cell windows were purged by nitrogen to remove air. This prevents formation of ozone due to the photodissociation of oxygen by ArF laser radiation and the interference from the transient absorption of ozone.

The residual light from the excimer laser pulse was removed using a spatial filter (1 mm diameter wire placed perpendicular to the slit in the focal spot of the second lens) and by a liquid filter (4.3×10^{-2} M solution NaCl in water, 1 cm). The liquid filter provides depression of 193 nm light 10^{12} times while attenuating the monitoring light (210.0 nm) only by about 20%. A photomultiplier tube (Hamamatsu R106) mounted on the exit slit operated on the reduced number of dynodes (6) with the voltage divider current of 2.7 mA, which ensured good linearity and lower noise at high photon fluxes. The PMT signal was preamplified (EMI preamplifier), then digitized and stored using

a digital storage oscilloscope (LeCroy 9310A, Dual channel, 400 MHz, 100 Msamples/s, 50 Kpts/ch). The time resolution was determined by the preamplifier settings. The time constants of 0.3 μs or 3 μs were used in the measurements. After the signal accumulation (ca. 300 pulses), the traces were transferred to a PC for processing.

A light shutter (Oriel Model 76993) was installed between the laser and the cell. Every even laser pulse was blocked. A synchronized switch (Pasternack Electronics, PE7100) was used to connect the two input channels of the oscilloscope to the preamplifier output to accumulate separately the light intensity profile with and without the laser pulse entering the reactor. This procedure was used to account for a small (0.5% in 1 ms) variation of the monitoring light intensity during a pulse. The two traces then were used to calculate the temporal profile of the monitoring light absorption.

The high-pressure flow system consisted of high-pressure mass flow controllers, a high-pressure flow cell, an upstream (back) pressure regulator, high-pressure test gauges, and cylinders with helium, the precursor, and the reactant mixtures. Brooks high-pressure mass flow controllers (5850 TR series) and Brooks electronic upstream pressure regulator (model 5866) were used. The flow controllers were periodically calibrated using the soap film method. The flow reactor pressure was measured using test pressure gauges (Matheson Model 63-5633M, up to 250 bar, Model 63-5622M, up to 14 bar, accuracy 0.25%) and by the internal calibrated pressure sensor of the electronic upstream pressure regulator.

Oxalyl chloride (98%, Aldrich Chem. Co.) was degassed by a freeze−pump−thaw procedure from liquid nitrogen. Then it was purified from a possible molecular chlorine impurity by pumping the vapor of an oxalyl chloride sample at temperature slightly above its melting point (−8 to −10 °C). After the oxalyl chloride degassing and purification, mixtures $(COCl)_2$/He of known compositions were prepared. When high-pressure (150 bar) mixtures were used, proper corrections for the nonideal behavior were introduced based on the tabulated compression factors.[28]

Phosgene (Matheson Inc.) was purified from molecular chlorine using three freeze−pump−thaw cycles. The low-temperature bath methanol-liquid N_2 (−98 °C) was used for freezing. Purified phosgene was premixed with helium. The content of molecular chlorine in the mixtures was evaluated using the absorption of molecular chlorine at 330 nm. The content of molecular chlorine in the purified phosgene was less than 0.13%.

Silane (3.1% mixture in He, semiconductor grade, purchased from Matheson) was used without further purification.

Helium from Matheson (UHP grade, 99.999%) was passed through an oxygen trap (R&D Separations, Model OT3-2) to ensure molecular oxygen content less than 0.02 ppm.

The photodepletion of oxalyl chloride by the ArF laser was measured using transient absorption at 210.0 nm (Zn HCL). The absorption cross-sections of silyl radical were measured at the 217.9 nm line of Cu HCL as well as at 206.4, 210.0, 213.9, 224.9, 231.9, 243.8, and 255.8 nm (Zn HCL).

Results and Discussion

The experiments were performed as follows. First, the photodepletion of oxalyl chloride due to the photodissociation caused by the ArF laser light is measured. The photodeplition is determined via the increase in the monitoring light intensity at $\lambda = 210.0$ nm, $\{\ln(I/I_0)\}_{OxCl,210}$. The measurements of oxalyl chloride were performed in the absence of silane twice, before and after the experiments with silane. The average of the results of the two measurements was used to calculate the initial concentration of chlorine atoms, and, subsequently, of silyl radicals, $[Cl]_0 = [SiH_3]_0$.

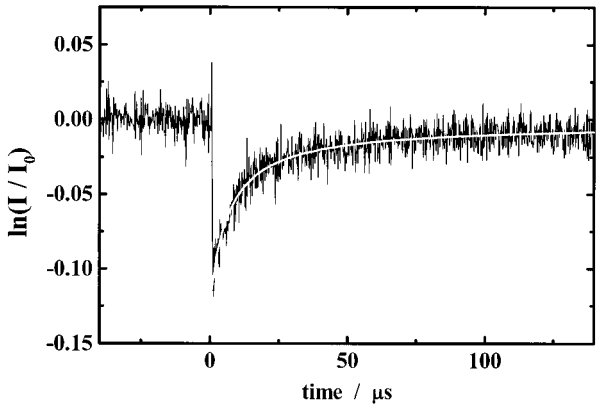

Figure 1. Transient absorption of SiH_3 radical at $\lambda = 213.9$ nm (Zn HCL). Line − fit with expression E2. The prompt increase in the absorption corresponds to the ArF laser pulse. $[(COCl)_2] = 4.5 \times 10^{15}$ molecule cm^{-3}; $[SiH_4] = 1.2 \times 10^{16}$ molecule cm^{-3}, $p_{He} = 1$ bar, $T = 303$ K.

An example of the temporal profile of the monitoring light absorption at 213.9 nm in a $(COCl)_2/SiH_4$/He mixture irradiated by a laser pulse is shown in Figure 1. The transient absorptions recorded with no silane added were subtracted from the transient absorptions recorded with addition of silane

$$\{\ln(I/I_0)\}_{corr} = \{\ln(I/I_0)\}_{[SiH4]} - \{\ln(I/I_0)\}_{[SiH4]=0} \quad \text{(E1)}$$

The temporal absorption profiles obtained in this way were fitted using the expression E2

$$\{\ln(I/I_0)\}_{corr} = -Abs_\infty - (Abs_0 - Abs_\infty)/(1 + 2\,Abs_0\,B\,t) \quad \text{(E2)}$$

This expression is derived under the assumption that the experimentally observed residual absorption at $t \rightarrow \infty$, Abs_∞, is caused by the products of reaction 1. The absorption caused by these products is assumed to appear instantaneously with the disappearance of silyl radicals on the time scale of the experiments. In this case, the initial absorption, Abs_0, and parameter B are expressed through the initial concentration of silyl radical, $[SiH_3]_0$, their absorption cross-section at the monitoring wavelength λ, $\sigma_{SiH3,\lambda}$, the reactor lengths, L, and the rate constant of reaction 1, k_1

$$Abs_0 = [SiH_3]_0\,\sigma_{SiH3,\lambda}\,L \quad \text{(E3)}$$

$$B = k_1/\sigma_{SiH3,\lambda}\,L \quad \text{(E4)}$$

The residual absorption, Abs_∞, was much smaller compared with the initial absorption, Abs_0. For example, in the experiment shown in Figure 1, the magnitude of the residual absorption is 7% of the initial absorption. The nature of the residual absorption and its pressure dependence are discussed later. The portion of the experimental curve in the interval 2−140 μs after the laser pulse was used to fit the data.

According to eq E2, no dependence of parameter B (defined in E4) on the initial concentration of silyl radicals is expected provided the interpretation is correct. The initial concentration of silyl radicals was varied via attenuation of laser radiation by insertion of partially transparent quartz plates. The dependence of the parameter B determined by the fitting of the experimental

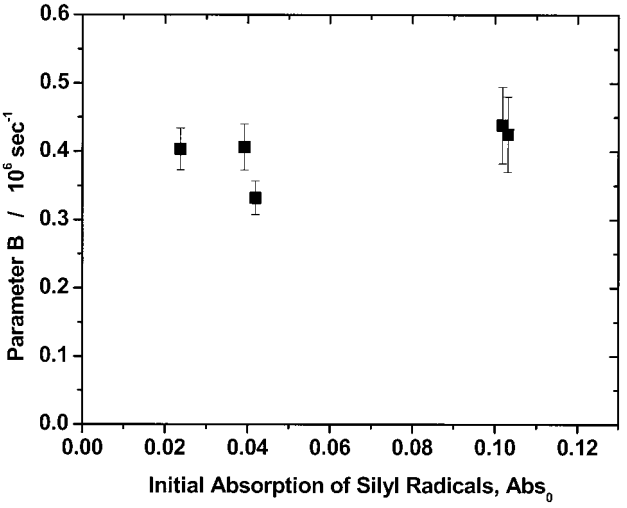

Figure 2. Parameter $B = k_1/\sigma_{SiH3,\lambda}\, L$ at $\lambda = 224.9$ nm (Zn HCL) plotted vs the initial absorption of silyl radicals. The initial concentration of silyl radicals is varied by the laser light attenuation. $[(COCl)_2] = 4.3 \times 10^{15}$ molecule cm^{-3}, $[SiH_4] = 2.9 \times 10^{16}$ molecule cm^{-3}, $p_{He} = 1$ bar, $T = 303$ K.

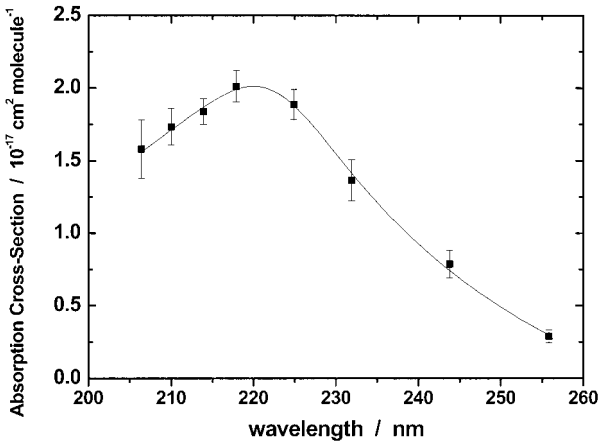

Figure 3. Absorption cross-section of SiH_3 vs wavelength. See text for details. Photodepletion of oxalyl chloride is determined via absorption at 210.0 nm. $[(COCl)_2] = (4.3-5.9) \times 10^{15}$ molecule cm^{-3}, $[SiH_4] = 3 \times 10^{16}$ molecule cm^{-3}, $p_{He} = 1$ bar, $T = 303$ K. Two measurements are taken at each wavelength, the average value is plotted.

TABLE 1: Absorption Cross-Section of Silyl Radical

wavelength (nm)	absorption cross-section (10^{-17}cm^2 molecule^{-1})
206.4	1.58 ± 0.20
210	1.73 ± 0.12
213.9	1.84 ± 0.09
217.9	2.01 ± 0.11
224.9	1.89 ± 0.11
231.9	1.36 ± 0.14
243.8	0.79 ± 0.10
255.8	0.29 ± 0.04

profiles obtained at different laser light intensities on the initial absorption of silyl radicals is shown in Figure 2. No dependence within the experimental error is observed, as expected based on the accepted model.

Absorption cross sections of silyl radical at different wavelengths are listed in Table 1 and plotted in Figure 3. In these measurements, the photodepleteion of oxalyl chloride was monitored through the absorption change at 210.0 nm in the absence of silane. Transient absorptions of silane were fitted by expression E2 to yield the initial absorption. The absorption cross-sections of silyl radical are calculated based on the

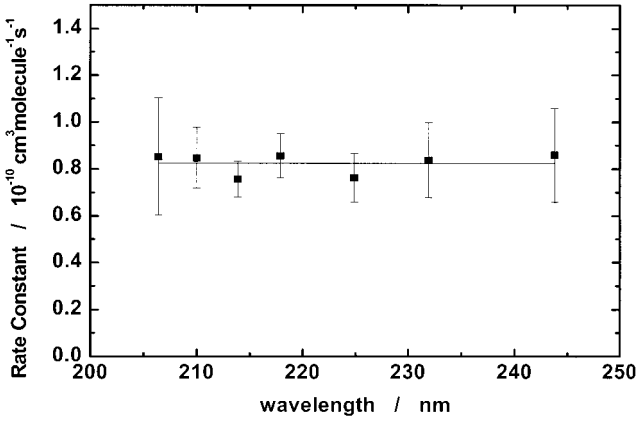

Figure 4. Rate constant of self-reaction of silyl radicals (reaction 1) measured at different monitoring light wavelengths. The same experimental data were used to determine the absorption cross-sections of silyl radical in Figure 3. $[(COCl)_2] = (4.3-5.9) \times 10^{15}$ molecule cm^{-3}, $[SiH_4] = 3 \times 10^{16}$ molecule cm^{-3}, $p_{He} = 1$ bar, $T = 303$ K. Two measurements are taken at each wavelength, the average value is plotted.

measured oxalyl chloride photodepletion, initial absorption of silyl radical, assuming the photodepletion yield of chlorine atoms of two and complete conversion of chlorine atoms to silyl radicals, $[Cl]_0 = [SiH_3]_0$. The shape of the absorption spectrum is in reasonable agreement with the relative spectrum reported by Lightfoot et al.[26] The absorption maxima and the long-wavelength parts are in good agreement. Lightfoot et al.[26] reported somewhat steeper fall of the absorption toward shorter wavelengths, compared with the results of the current work. Although the absolute cross section was not determined due to the uncertainty in the chlorine atom yield in photolysis of CCl_4 by broad-band flash lamp light, the possible range of the cross-section was given as $1.4 \times 10^{-17} - 2.4 \times 10^{-17}$ cm^2 molecule^{-1}.[26] The absolute absorption cross-section in the maximum determined in this work, $(2.01 \pm 0.11) \times 10^{-17}$ cm^2 molecule^{-1} is in agreement with this prediction.

The rate constant of self-reaction of silyl radicals 1 was obtained based on the measured parameters $B = k_1/\sigma_{SiH3,\lambda}L$ and the absorption cross-sections of the radical, $\sigma_{SiH3,\lambda}$. Figure 4 shows the rate constant obtained in this way as a function of the monitoring light wavelength used in the measurements at helium buffer gas pressure 1 bar. No dependence of the rate constant on the monitoring wavelength within the experimental error is observed, which indicates the correctness of the data interpretation. The average value (solid line in Figure 4) yields $k_1 = (8.25 \pm 0.35) \times 10^{-11}$ cm^3 molecule^{-1} s^{-1} (the error indicated is one standard deviation). With all experimental errors, the measured value is $k_1 = (8.25 \pm 1.05) \times 10^{-11}$ cm^3 molecule^{-1} s^{-1}

The residual absorption which exists at long times compared to self-reaction of silyl radicals was assigned to the products of reaction 1. The spectrum of this residual absorption is shown in Figure 5. The data in Figure 5 were obtained at the buffer gas pressure 1 bar. The most probable species responsible for this absorption is disilene, H_2SiSiH_2, formed in the process of isomerization of energized $HSiSiH_3$ produced in reaction 1c

$$HSiSiH_3^* \rightarrow H_2SiSiH_2 \qquad (5)$$

Silenes have strong absorption in the far UV.[29] Matsumoto et al.[23] determined that at low pressures molecular hydrogen is produced in the self-reaction of SiH_3 radicals with the yield of $11 \pm 4\%$. On the basis of the yield of molecular hydrogen, the branching ratio for the dissociation of the energized disilane

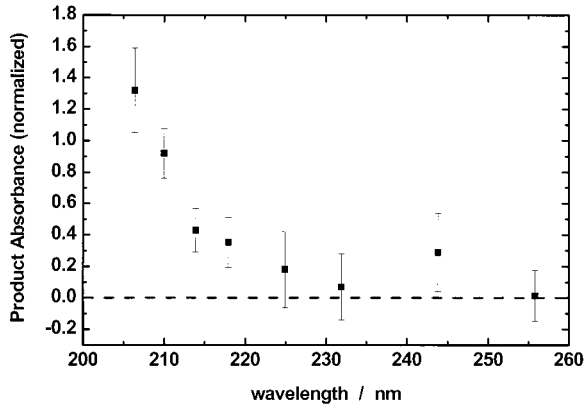

Figure 5. The relative spectrum of the residual absorption (parameter Abs_∞ in the fitting expression E2, the absorption surviving at long times, attributed to the absorption of the products of reaction 1), normalized on the value of photodepletion of the oxalyl chloride absorption at 210 nm. The same experimental data were used to determine the absorption cross-sections of silyl radical in Figure 3. $[(COCl)_2] = (4.3-5.9) \times 10^{15}$ molecule cm^{-3}, $[SiH_4] = 3 \times 10^{16}$ molecule cm^{-3}, $p_{He} = 1$ bar, $T = 303$ K.

molecule formed in reaction 1a was estimated as $k_{1c}/(k_{1c}+k_{1b}) = 0.19$. Disilane molecules formed in recombination of silyl radicals (1a) have ca. 20 kcal mol^{-1} energy in excess of that required for the dissociation via channel 1c. According to the recent G2 calculations, reaction 5 is exothermic ($\Delta H_{298} = -7.3$ kcal mol^{-1}), with the barrier to isomerization of 7.5 kcal mol^{-1}.[30] Therefore, a fast reaction 5, which converts a transient species into a relatively stable molecule containing a double bond, is feasible.

It could be also argued by analogy with silylene that the insertion of $SiHSiH_3$ into SiH_4 should be relatively fast. This process would lead to formation of Si_3H_8, which might be another possible candidate for the residual absorption. However, based on the amplitude of the residual absorption and the fraction of channel 1c, the absorption cross-section of the species responsible for the residual absorption must be relatively large ($> 2 \times 10^{-17}$ cm^2 molecule^{-1}). It seems to be improbable for a small Si/H-containing species with saturated bonds to have such strong absorption at wavelengths longer than 200 nm. Monosilane, SiH_4, has absorption band of a comparable strength at much shorter wavelength (ca. 150 nm[31]).

Because the residual absorption is attributed to the primary and secondary products of dissociation of energized Si_2H_6 molecules, it is expected to be pressure dependent. At elevated pressures the stabilization channel 1d is expected to compete with the dissociation channel 1c. The stabilization product (disilane, Si_2H_6), does not absorb at $\lambda > 200$ nm. Therefore, the residual absorption is expected to be "quenched" by the buffer gas pressure.

The absorption cross-section of silyl radicals at a single wavelength, 224.9 nm, was measured over the buffer gas pressure range, 1−100 bar. No pressure dependence of the absorption cross section of SiH_3 was found within the experimental error (Figure 6). This could be expected in view of the broad structureless nature of the absorption band of silyl radical in the UV.

The pressure dependence of the residual absorption at 210.0 nm is shown in Figure 7. As expected, the amplitude of the residual absorption decreases with pressure. This corroborates the interpretation of the residual absorption as being caused by the Si_2H_6* dissociation products of reaction 1. The residual absorption is suppressed almost completely at 100 bar helium pressure, which infers that the stabilization channel 1d almost

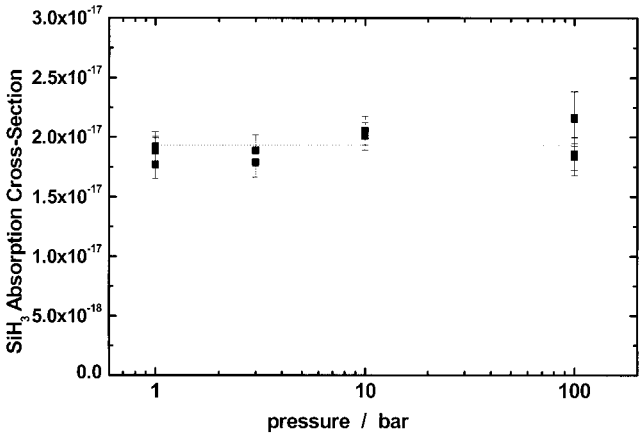

Figure 6. Absorption cross-section of SiH_3 at $\lambda = 224.9$ nm (Zn HCL) vs the buffer gas pressure. $[(COCl)_2] = (4.3-5.9) \times 10^{15}$ molecule cm^{-3}, $[SiH_4] = (3-9) \times 10^{16}$ molecule cm^{-3}, $T = 297-303$ K.

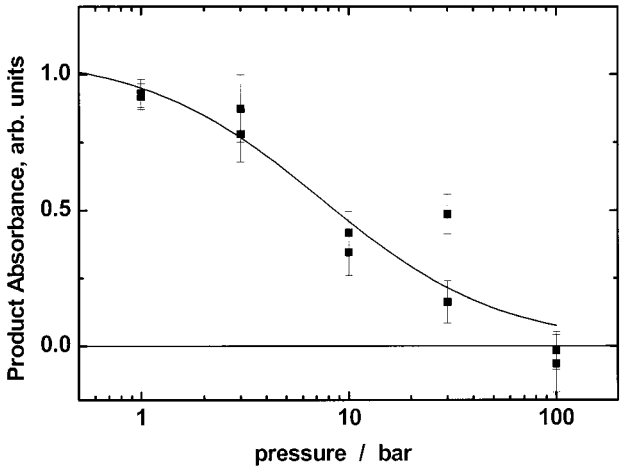

Figure 7. Pressure dependence of the residual absorption (the absorption surviving at long times) attributed to the products of SiH_3 self-reaction measured at 210.0 nm. $[(COCl)_2] = (5.2-6.4) \times 10^{15}$ molecule cm^{-3}, $[SiH_4] = (4-17) \times 10^{16}$ molecule cm^{-3}, $T = 297$ K. The line is the fit by expression E5 (see text).

completely dominates in the reaction mechanism at ambient temperature and pressure 100 bar.

The solid curve in Figure 7 is obtained by the fitting of the experimental data with the expression E5

$$\phi = (1 + p/p_{1/2})^{-1} \qquad \text{(E5)}$$

Such a dependence is expected for quenching of dissociation channels of chemically activated molecules[32]

$$\phi = (1 + \gamma_c Z_{LJ}[He]/k(E^+))^{-1} \qquad \text{(E6)}$$

where ϕ is the relative yield of the dissociation product, γc is the "weak collizion efficiency" for a chemically activated system, Z_{LJ} is the Lennard−Jones binary collision number, [He] is the number density of the buffer gas (He), E^+ is the excess energy of the enegized Si_2H_6 molecule above the dissociation level, and $k(E^+)$ is the rate constant of dissociation of energized Si_2H_6* molecules.[32]

The fit yielded $p_{1/2} = 8.5 \pm 2.0$ bar. Using the estimated Lennard−Jones collision frequency, $Z_{LJ} = 5.6 \times 10^{-10}$ cm^3 molecule^{-1} s^{-1}, and $k(E^+) = k_{1c}(E^+) + k_{1b}(E^+) = 2.9 \times 10^{10}$ s^{-1},[23] this leads to $\gamma_c = 0.25$. The dissociation rate constant for the energized disilane molecule was estimated by RRKM calculations[23] with the transition state suggested for the thermal

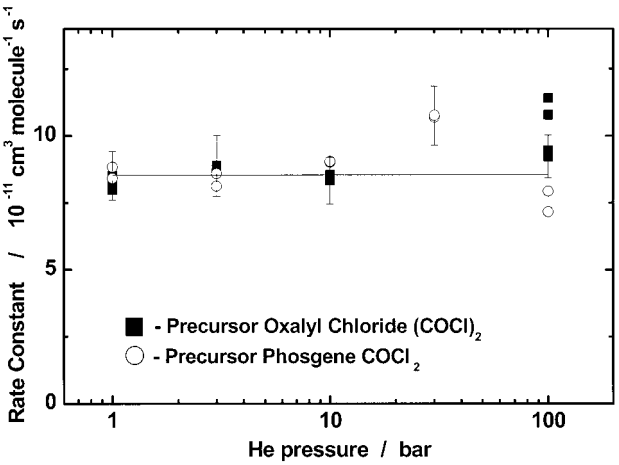

Figure 8. Pressure dependence of the rate constant of self-reaction of SiH_3 radicals (reaction 1) measured at the wavelength $\lambda = 224.9$ nm (Zn HCL). ■- Oxalyl chloride, $(COCl)_2$, is used as a precursor of chlorine atoms, the experimental condition as in Figure 6. O−phosgene, $COCl_2$, is used as a precursor. $[COCl_2] = 3.1 \times 10^{16}$ molecule cm^{-3}, $[SiH_4] = (3-15) \times 10^{16}$ molecule cm^{-3}, $T = 294-297$ K.

decomposition of disilane.[33] This value, although somewhat (ca. 2−4 times) larger than that which could be expected assuming the energy transferred in collisions with He atoms of 2 kJ mol^{-1},[34] should be considered as reasonable given the uncertainties associated with the thermochemistry and the RRKM theory.[23,34]

It should be noted, that if silylene formed in reaction 5 is the major absorbing species causing the residual absorption, then the observed pressure quenching of the residual absorption can be due both to the collisional vibrational relaxation of energized disilane molecules (1d) and collisional relaxation of excited $HSiSiH_3$ produced in reaction 1c.

The rate constant of reaction 1 was measured at different bath gas (He) densities over the range 1−100 bar. The results are shown in Figure 8. No pressure dependence was observed within the experimental error. Two photolytic sources of chlorine atoms—oxalyl chloride, $(COCl)_2$, and phosgene, $COCl_2$—were used. The data obtained with two different precursors of chlorine atoms are in excellent agreement. The points at elevated pressures (30 and 100 bar) have larger error and were not used to derive the average value of the rate constant. The average rate constant obtained by averaging the low buffer pressure data, $(8.55 \pm 0.35) \times 10^{-11}$ $cm^3 molecule^{-1} s^{-1}$ ($\pm$ 1 st. dev.), is in excellent agreement with the rate constant obtained at 1 bar using different monitoring light wavelengths. These measurements, in turn, are in good agreement with the previous determination of Loh an Jasinski, $(7.9 \pm 2.9) \times 10^{-11}$ cm^3 $molecule^{-1} s^{-1}$.

Conclusion

The rate constant of self-reaction of silyl radicals was remeasured using two precursors of chlorine atoms—oxalyl chloride and phosgene. Oxalyl chloride, $(COCl)_2$, was recently suggested as a new clean photolytic precursor of chlorine atoms.[25] Absolute absorption cross-section of silyl radicals was determined as a function of wavelength. Rate constants of reaction 1 was measured at different wavelengths and the buffer gas pressure. The measurements at different experimental conditions yielded consistent results in excellent agreement with the value reported by Loh and Jasinski.[20] The reason for the low value of the rate constant obtained using phosgene as a precursor of chlorine atoms in an earlier study[22] is not resolved.

Acknowledgment. This work was supported by the Petroleum Research Fund administered by the American Chemical Society (Grant No. 31640-AC6).

References and Notes

(1) Jasinski, J. M.; Meyerson, B. S.; Scott, B. A. *Annu. Rev. Phys. Chem.* **1987**, *38*, 109.
(2) Kapoor, V. J.; Stein, H. J. *Silicon Nitride Thin Insulating Films*; Symposium Proceedings; The Electrochemical Society, Inc.: Pennington, NJ, 1983. Vol. 83−8.
(3) Belyi, V. I.; Vasilyeva, L. L.; Ginovker, A. S.; Gritsenko, V. A.; Repinsky, S. M.; Sinitsa, S. P.; Smirnova, T.; Edelman, F. L. *Silicon Nitride in Electronics*; Materials Science Monographs; Elsevier: Amsterdam, 1988. Vol. 34.
(4) Krasnoperov, L. N.; Braun, V. R.; Nosov, V. V.; Panfilov, V. N. *Kinetics and Catalysis.* **1981**, *22*, 1049.
(5) Braun, V. R.; Krasnoperov, L. N.; Panfilov, V. N. *Proc. of the Academy of Sciences of USSR.* **1981**, *260*, 876.
(6) Braun, V. R.; Krasnoperov, L. N.; Panfilov, V. N. *Khim. Fizika.* **1982**, *6*, 758.
(7) Braun, V. R.; Krasnoperov, L. N.; Panfilov, V. N. *Oxidation Communications.* **1984**, *6*, 259.
(8) Krasnoperov, L. N.; Chesnokov, E. N.; Panfilov, V. N. *Chem. Phys.* **1984**, *89*, 297.
(9) Chasovnikov, S. A.; Krasnoperov, L. N. *Khim. Fizika*. **1987**, *6*, 956.
(10) Jasinski, J. M.; Becerra, R.; Walsh, R. *Chem. Rev.* **1995**, *95*, 1203.
(11) Seetula J. A.; Feng Y.; Gutman D.; Seakins P. W.; Pilling, M. J. *J. Phys. Chem.* **1991**, *95*, 1658.
(12) Kalinovski, I. J.; Gutman, D.; Krasnoperov, L. N.; Goumri, A.; Yuan, W.-J.; Marshall, P. *J. Phys. Chem.* **1994**, *98*, 9551.
(13) Krasnoperov, L. N.; Niiranen, J. T.; Gutman, D.; Melius, C. F.; Allendorf, M. D. *J. Phys. Chem*. **1995**, *99*, 14 347.
(14) Krasnoperov, L. N.; Kalinovski, I. J.; Niiranen, J. T.; Gutman, D. *J. Phys. Chem. A*. **1997**, *101*, 4929.
(15) Becerra, R.; Walsh, R. *J. Phys. Chem*. **1987**, *91*, 5765.
(16) Itabashi, N.; Kato, K.; Nishiwaki, N.; Goto, T.; Yamada, C.; Hirota, E. *Jpn. J. Appl. Phys*. **1989**, *28*, PL 325.
(17) Niki, H.; Maker, P. D.; Savage, C. M.; Breitenbach, L. P. *J. Phys. Chem*. **1985**, *89*, 1752.
(18) Chasovnikov, S. A.; Krasnoperov, L. N. *Kinetics and Catalysis* (Eng. Trans.). **1990**, *31*, 1125.
(19) Loh, S. K.; Beach, D. B.; Jasinski, J. M. *Chem. Phys. Lett*. **1990**, *55*, 169.
(20) Loh, S. K.; Jasinski, J. M. *J. Chem. Phys*. **1991**, *95*, 4914.
(21) Koshi, M.; Miyoshi, A.; Matsui, H. *J. Phys. Chem*. **1991**, *95*, 9869.
(22) Baklanov, A. V.; Chichinin, A. T. *Chem. Phys*. **1994**, *181*, 119.
(23) Matsumoto, K.; Koshi, M.; Okawa, K.; Matsui, H. *J. Phys. Chem*. **1995**, *100*, 8796.
(24) Sugawara, K.; Nakanaga, T.; Takeo, H.; Matsumura, C. *Chem. Phys. Lett*. **1989**, *157*, 309.
(25) Baklanov, A. V.; Krasnoperov, L. N. *J. Phys. Chem*. **2001**, *105*, 97.
(26) Lightfoot, P. D.; Becerra, R.; Jemi-Alade, A. A.; Lesclaux, R. *Chem. Phys. Lett*. **1991**, *180*, 441.
(27) Krasnoperov, L. N.; Mehta, K. *J. Phys. Chem. A.* **1999**, *103*, 8008.
(28) *International Thermodynamic Tables of the Fluid State. Helium-4.* IUPAC Division of Physical Chemistry Commission on Thermodynamics and Thermochemistry Thermodynamics Tables Project; Angus, S., de Reuck, K. M., McCarty, R. D., Eds; Pergamon Press: New York, 1977.
(29) Brix, Th.; Arthur, N. L.; Potzinger, P. *J. Phys. Chem.* **1989**, *93*, 8193.
(30) Swihart, M. T.; Carr, R. W. *J. Phys. Chem. A.* **1998**, *102*, 785.
(31) Robin, M. B. *Higher Excited States of Polyatomic Molecules, v.1*. **1974**, AP, NY, p 298.
(32) Troe, J. *J. Phys. Chem.* **1983**, *87*, 1800.
(33) Moffat, H. K.; Jensen, K. F.; Carr, R. W. *J. Phys. Chem.* **1992**, *96*, 7683.
(34) Gardiner, W. C., Jr.; Troe, J. *Rate Coefficients of Thermal Dissociation, Isomerization, and Recombination Reactions.* In: *Combustion Chemistry*, Ed. Gardiner W. C., Jr. Springer-Verlag: New York, 1984. p 173−196.